

# Feasibility of Software-Based Real-Time Calibration of Multi-Gigabit PET Data

D. L. Freese, *Student Member, IEEE*, D. F. C. Hsu, *Student Member, IEEE*, D. Innes,  
and Craig S. Levin, *Member, IEEE*

**Abstract**—Positron Emission Tomography (PET) imaging of the breast has the potential to play a role in the detection, diagnosis, staging, guiding surgical resection, and monitoring of therapy for breast cancer. Of these potential roles, producing images at near or real-time is especially important to guide surgical resection and biopsy. This task becomes more difficult in systems with large numbers of detectors and channels. We are constructing a two-panel clinical PET system dedicated to imaging the breast that has 294,912 LYSO crystals read out by 4608 Position-Sensitive Avalanche Photodiodes (PSAPD). The system will read out data using UDP over six gigabit ethernet ports with a maximum predicted data rate of 456MBps for clinical settings. We discuss software considerations for receiving data since UDP does not guarantee transmission. We implement a dual-threaded design for receiving then processing raw data from the system. This model shows  $0.037 \pm 0.004$  % data loss at 240MBps. This rate is the maximum for the current two gigabit ethernet cable setup. We extend and test data loss of the dual-threaded model by adding additional processing of raw data in the second thread. The processing of raw data produces calibrated data with an accurate timestamp, energy, and position in real-time. We show negligible ( $< 0.0001$  %) loss at or below 60MBps. There, however, is a steady increase in loss with increasing data rate up to  $45.9 \pm 0.6$  % loss at 240MBps. We conclude, that barring upgrades to our current data acquisition computer, we need to produce calibrated data from saved raw data after the scan, which can be done quickly without the constraint of minimizing data loss.

## I. INTRODUCTION

POSITRON Emission Tomography (PET) imaging of the breast has the potential to play a role in the detection, diagnosis, staging, guiding surgical resection, and monitoring of therapy for breast cancer [1]. Of these potential roles, producing images at near or real-time is especially important to guide surgical resection and biopsy. This, however, becomes more difficult when dealing with systems that have a large number of active components, as the required calibration steps increase.

To address the operational challenges of complex systems, some groups have employed sophisticated monitoring systems

D. L. Freese, D. F. C. Hsu, and C. S. Levin are with the Department of Electrical Engineering, Stanford University, Stanford, CA, 94305 USA e-mail: dfreese@stanford.edu.

D. Innes, and C. S. Levin are with the Department of Radiology at Stanford University.

C. S. Levin is also with the Departments of Physics and Bioengineering at Stanford University

D. L. Freese is supported by a Stanford Graduate Fellowship and a National Science Foundation Fellowship.

Manuscript received May 31st, 2016.

to allow the operator to monitor the performance of the system [2]. On the computational side, other groups have built upon parallel processing techniques to address the problem of calibrating data for using in coincidence sorting and image reconstruction for PET systems that readout raw ADC channel data [3]–[5]. Furthermore, the stability of the different parameters used in the calibration begins to play an important role, as filtering steps performed on the data can remove good data due to incorrect calibration information [6].

We have constructed one third of a PET system for loco-regional imaging, with a focus on the breast. The system in its final form it will contain 294,912 LYSO crystals read out by 4608 Position-Sensitive Avalanche Photodiodes (PSAPD) and will require 907,776 parameters to be measured in order to produce singles event data with accurate time, energy, and position. The DAQ system is controlled by FPGAs which send raw ADC channel data to a data acquisition computer over gigabit ethernet links using the User Datagram Protocol (UDP) [7]. Currently the design has two gigabit ethernet cables, but six are planned for the final design. We have previously implemented data acquisition (DAQ) software for the purposes of online monitoring of the system [8].

In this work, we examine the feasibility of producing calibrated event data in real-time. First, the software structure required to minimize data loss is examined. Next, the effect of additional processing steps is covered, and finally we study the measured calibration stability and discuss the implications of this for producing an image in real time.

## II. SOFTWARE DESIGN

For our system, UDP/IP was used as a sending protocol from the FPGAs, as it is stateless, and therefore requires significantly fewer resources to implement using an FPGA that uses TCP/IP. A downside of this design choice is UDP does not guarantee the data is received, and can be silently dropped by the receiving computer. The DAQ software therefore must be designed to minimize data loss. Computational time spent outside of monitoring the incoming port increases the chances that a UDP packet will be dropped. For this reason we use the two thread design shown in Figure 1. This allows one of the threads to continuously monitor an ethernet port, while the other can write to disk or do additional processing. The transfer buffer is capped at 100MB, and since this is a multi-threaded program, access to the transfer buffer is protected by a mutual-exclusion, or mutex, lock to protect from conflicting reads and writes. To ensure that the receiving thread does not

lose time waiting to lock the transfer buffer, it will only place data in the buffer if it is not locked by the other thread.

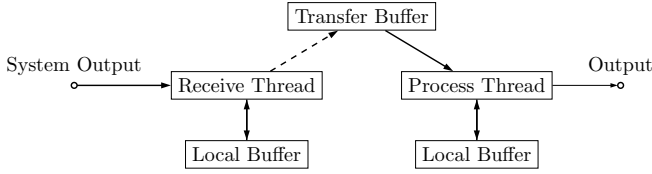


Fig. 1. The software thread structure chosen to minimize data loss. The dashed line indicates the receive thread will not wait for the transfer buffer if it is locked by the process thread.

We tested this software design against a single thread design, where one thread monitors the port then immediately writes it to disk on a 4 core Intel i7-4771 with 16GB RAM. In this experiment we used a standard linux networking socket with a 25MB buffer. By default, the Linux kernel has a much smaller default and max buffer size, which shows consistent loss across all data rates. At each data rate shown, data was collected for 120s and the resulting data loss was evaluated. The experiment was repeated 7 times and the standard error was calculated. In our experiments the linux networking stack caused a consistent and considerable data loss, even at low data rates. Our experiments, as seen in Figure 2 show non-negligible and increasing loss for the single thread mode, but negligible loss for the dual-thread model. As a technical note, atomic variables, which enforce sequential and thread-safe reading of a variable were used inside all threads to synchronize the starting, stopping, and write-out. These were implemented using the GNU C++ standard library. Atomic variables in GCC versions prior to 4.7 caused an order of magnitude jump in data loss due to their use of mutex locks in their implementation. The performance of this design scales well with the addition of a second ethernet port. With the two ethernet ports in our current setup sending at a full capacity (240MBps), this structure allows for data to be received and written to disk with a data loss of  $0.037 \pm 0.004\%$  as seen later in Figure 4. Error bars represent standard error over 3 trials for 5 min. The maximum data rate we expect in a clinical setting based on simulations from six ethernet ports would be 456MBps [9].

### III. ONLINE CALIBRATION OF DATA

We showed that the multi-threaded structure is able to reliably capture almost all UDP data sent by the system. We now examine the impact of adding additional processing of the data prior to writing it to disk. There are several steps that need to be taken to go from the raw data stream sent from the system to a calibrated event, as seen in Figure 3.

The decoding of channel information parses the raw data stream for packets from the FPGA representing a trigger on one or more of the PSAPDs, and rejects any malformed data. Next, the measured DC offsets to the ADC channels, or pedestals, are subtracted from the measured channel value. This allows for coarse energy thresholds to be applied to each event. The X and Y position of the event along the face of

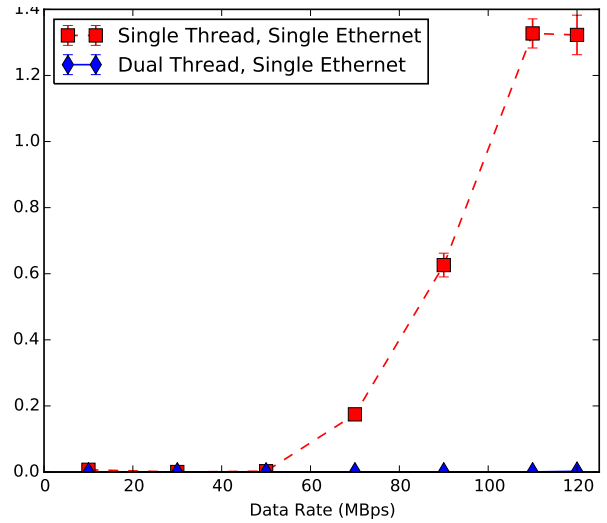


Fig. 2. The graph above shows the benefit of each software design choice for receiving a UDP data stream and writing it to a disk. The dual-thread model, seen in Figure 1, shows a clear benefit of over the single thread model. 120MBps represents the maximum of one port, including UDP overhead.

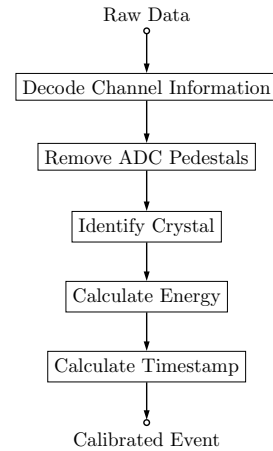


Fig. 3. The steps required to produce an event with a calibrated time, energy, and position.

the PSAPD is calculated using Anger logic. This position is then compared to the stored location of each of the 64 crystals for the PSAPD and assigned to the crystal with the closest euclidean distance, requiring 64 distance calculations. The energy of the event is then calculated using the crystal's stored 511 keV photopeak position, and finally the timestamp of the event, which is energy dependent, can be calculated. Sorting of the events can be efficiently done using an insertion sort algorithm, as they are already mostly sorted to begin with. The results of performing these operations in real-time for a 5 min test with two gigabit ethernet cables can be seen in Figure 4. We show negligible ( $< 0.0001\%$ ) loss at or below 60MBps. Afterwards, Data loss increases with data rate up to  $45.9 \pm 0.6\%$  loss at 240MBps. An order of magnitude increase in buffer size only marginally decreases the observed loss, thus calibration appears to be limited by the computational power of a single processing thread.

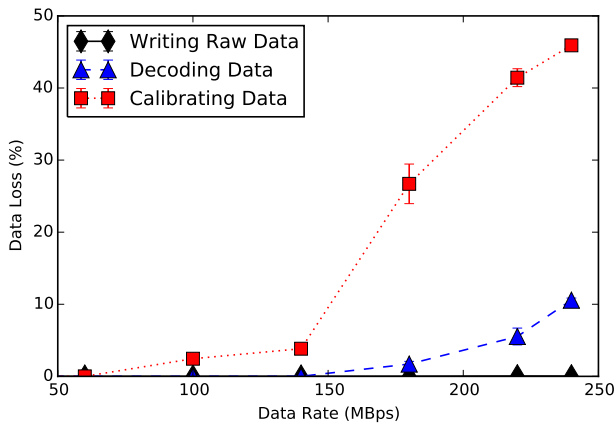


Fig. 4. The impact on data loss of additional computation beyond writing raw data to disk. The data rate represents the total combined rate. Losses at 60MBps and below are negligible.

#### IV. CALIBRATION STABILITY

The calibration process described in the previous section relies on a stored calibration parameters to be able to calculate the final output. The stability of these parameters effects the resulting image quality and the events are kept or rejected, which is of importance to this work. Additionally, it contains two non-linear processes, anger logic and an arctan operation to calculate a phase angle that is used for timing. If these parameters are stable then the raw data can be discarded. If not, then the raw values must be stored so any errors can be corrected after a scan.

Pedestal values show a standard deviation of  $12.5 \pm 0.1$  adc channels, or  $10.4 \pm 0.1$  keV, across 8 measurements, however, they can be measured accurately in under 5s, so these can be measured prior to every scan to avoid this inaccuracy. The 511 keV photopeak position for each crystal within the system is another parameter that must be estimated from the incoming data. Seven scans of a  $^{22}\text{Na}$  point source were made over a period of several days, and the 511 keV photopeak position in ADC units was estimated for each crystal for every scan. The distribution of all of the photopeak positions for each crystal is shown in Figure 5. For clarity, all of the values have been normalized to 511 keV by the mean of the crystal to account for the different crystal gains. As a result, the energy window for the system will need to be widened by 25 keV to accommodate crystals with a larger variation. The deviation of the parameters used for the phase angle calculation would contribute at most 0.2 ns FWHM to the timing resolution of the system, so the raw data can be dropped.

#### V. CONCLUSIONS

In this work we investigated the feasibility of performing software-based calibration of raw data from a PET system dedicated to imaging the breast. We demonstrate the ability to store raw data from our system with a loss of  $0.037 \pm 0.004$ %. For data rates at or below 60MBps, we are able to calibrate, sort, and energy gate the raw data from our system in real-time with negligible ( $< 0.0001$ %) loss. We do this using a

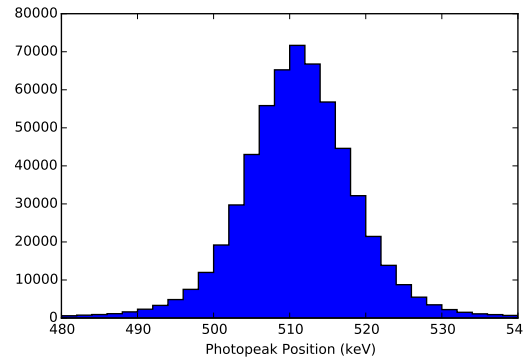


Fig. 5. Distriution of crystal 511 keV photopeak positions across seven scans.

dual-threaded design of receiving and processing that shows a factor of 60 improvement in data loss from a single threaded program. There, however, is a steady increase in loss with increasing data rate up to  $45.9 \pm 0.6$ % loss at 240MBps. We conclude, that barring upgrades to our current data acquisition computer, we need to produce calibrated data from saved raw data after the scan, which can be done quickly without the constraint of minimizing data loss.

#### REFERENCES

- [1] D. F. C. Hsu, D. L. Freese, and C. S. Levin, "Breast-dedicated radionuclide imaging systems," *Journal of Nuclear Medicine*, vol. 57, no. Supplement 1, pp. 40S–45S, 02 2016. [Online]. Available: [http://jnm.snmjournals.org/content/57/Supplement\\_1/40S.abstract](http://jnm.snmjournals.org/content/57/Supplement_1/40S.abstract)
- [2] J. Charest, J. F. Beaudoin, J. Cadorette, R. Lecomte, C. A. Brunet, and R. Fontaine, "Automatic channel fault detection on a small animal apd-based digital pet scanner," *Nuclear Science, IEEE Transactions on*, vol. 61, no. 5, pp. 2494–2502, Oct. 2014.
- [3] D. P. McElroy, M. Hoose, W. Pimpl, V. Spanoudaki, T. Schüler, and S. I. Ziegler, "A true singles list-mode data acquisition system for a small animal pet scanner with independent crystal readout," *Physics in Medicine and Biology*, vol. 50, no. 14, p. 3323, 2005. [Online]. Available: <http://stacks.iop.org/0031-9155/50/i=14/a=009>
- [4] R. Fontaine, F. Belanger, N. Viscogliosi, H. Semmaoui, M. A. Tetrault, J. B. Michaud, C. Pepin, J. Cadorette, and R. Lecomte, "The hardware and signal processing architecture of labpet&#x2122;, a small animal apd-based digital pet scanner," *Nuclear Science, IEEE Transactions on*, vol. 56, no. 1, pp. 3–9, Feb. 2009.
- [5] B. Goldschmidt, C. W. Lerche, T. Solf, A. Salomon, F. Kiessling, and V. Schulz, "Towards software-based real-time singles and coincidence processing of digital pet detector raw data," *Nuclear Science, IEEE Transactions on*, vol. 60, no. 3, pp. 1550–1559, June 2013.
- [6] C. W. Lerche, J. Mackewn, B. Goldschmidt, A. Salomon, P. Gebhardt, B. Weissler, R. Ayres, P. Marsden, and V. Schulz, "Calibration and stability of a sipm-based simultaneous pet/mr insert," *Nuclear Instruments and Methods in Physics Research Section A: Accelerators, Spectrometers, Detectors and Associated Equipment*, vol. 702, pp. 50–53, 2 2013. [Online]. Available: <http://www.sciencedirect.com/science/article/pii/S0168900212009126>
- [7] P. D. Reynolds, F. W. Y. Lau, A. Vandenbroucke, and C. S. Levin, "Readout design and validation for a 1 mm<sup>3</sup> resolution clinical pet system," *Nuclear Science Symposium Conference Record (NSS/MIC), 2010 IEEE*, pp. 3097–3099, 2010.
- [8] U. Yoruk, A. Vandenbroucke, P. Reynolds, and C. Levin, "Design and implementation of scalable daq software for a high-resolution pet camera," in *Nuclear Science Symposium and Medical Imaging Conference (NSS/MIC), 2012 IEEE*. IEEE, 2012, pp. 2537–2539.
- [9] A. Vandenbroucke, D. Innes, and C. S. Levin, "Effects of external shielding on the performance of a 1 mm<sup>3</sup> resolution breast PET camera," *Nuclear Science Symposium Conference Record (NSS/MIC), 2010 IEEE*, pp. 3644–3648, Oct. 30 2010–Nov. 6 2010.